Multivariable Quadratic Synthesis of an Advanced Turbofan Engine Controller

R.L. DeHoff* and W.E. Hall Jr.†
Systems Control, Inc. (Vt.), Palo Alto, Calif.

A digital controller for an advanced turbofan engine utilizing multivariate feedback is described. The theoretical background of locally linearized control synthesis is reviewed briefly. The application of linear quadratic regulator techniques to the practical control problem is presented. The design procedure has been applied to the F100 turbofan engine, and details of the structure of this system are explained. Selected results from simulations of the engine and controller are utilized to illustrate the operation of the system. It is shown that the general multivariable design procedure will produce practical and implementable controllers for modern, high-performance turbine engines.

Nomenclature

A = trim switching matrix
A = quadratic state weighting matrix
A_j = nozzle area
B = quadratic control weighting matrix
C = feedback gain matrix
D = linearized measurement matrix
f = nonlinear engine model
F = linearized engine dynamics matrix
H = linearized measurement matrix
H = Hamiltonian matrix
h = nonlinear measurement function
h = a row of the H matrix
n = number of states
N = rotor speed
m = number of controls
P_3 = burner pressure
$P_{4.5}$ = interturbine volume pressure
P_6 = augmentor entrance pressure
p = number of outputs
q = number of parameters
r = number of possible trim variables
S = steady-state Ricatti matrix
T = state transformation matrix
$T_{2.5H}$ = fan exit inner temperature
$T_{2.5C}$ = fan exit outer temperature
T_3 = compressor discharge temperature
T_{4HI} = high turbine inlet temperature, high response
T_{4LO} = high turbine inlet temperature, low response
T_4 = high turbine inlet temperature, local
$T_{4.5HI}$ = fan turbine inlet temperature, high response
$T_{4.5LO}$ = fan turbine inlet temperature, low response
T_5 = fan turbine exit temperature
T_{6C} = augmentor entrance temperature
T_{7M} = augmentor exit temperature
u = $m \times 1$ control vector
x = $n \times 1$ state vector
y = $p \times 1$ output vector
z = modal coordinate
θ = vector of parameters
δ = perturbation quantity
$\Delta p/p$ = fan exit Mach number parameter
Λ = block diagonal matrix
$\equiv$ = modal controllability matrix
λ_j = eigenvalue

Received July 15, 1977; revision received Sept. 2, 1977.

Index categories: Guidance and Control; Airbreathing Propulsion.

*Senior Engineer, System Identification and Control Division. Member AIAA.

†Program Manager, System Identification and Control Division. Member AIAA.

Introduction

MODERN aircraft turbine engine designs provide the controls engineer with a variety of sensors and actuators for use in transient and steady-state operations. Classical designs have relied on hydromechanical fuel controls, i.e., a speed governor for gross transient response with more sophisticated control action used in steady-state regulation and trim. The incorporation of digital processing capability into the system allows an integrated control action to meet steady-state and transient performance requirements. It thus is possible to apply linear, quadratic regulator synthesis theory to the design of multivariable engine digital control system for operation throughout the flight envelope. The advantages of such procedures include 1) enhanced performance from cross-coupled controls, 2) maximum use of engine variable geometry, and 3) a systematic design procedure that is applied efficiently to new engine systems.

Development of multivariate or interactive control systems for modern turbojet, turbofan, and advanced cycle engines has been a highly active field since the incorporation of the first practical digital controller into a modern aircraft turbine engine, viz the F100. Stone et al.[1] have presented an approach to optimal control for the J85 turbojet engine. Seitz[2] has incorporated a simplified J85 dynamical model with a phugoid approximation to F-4 longitudinal motion in the design of a coupled autothrottle system. Michael and Farrar[3] present an analytical formulation for the engine transient regulation problem. Beattie[4] has explored various practical coupled control modes for future variable-geometry engines. The F100 turbofan engine presents a more complex dynamical behavior than the essentially first-order response of the J85 turbojet. Weinberg[5] and Merril[6] have reported various advanced digital control formulations for sea-level static conditions. Teren[7] has investigated open-loop optimal inputs for minimum-acceleration time transients. The authors[8,9] have presented a practical multivariable control procedure for full envelope operation of the F100. The structure and behavior of this system is described presently. A more detailed presentation of the results of the program is available in Refs. 10 and 11.

Theoretical Synthesis Method

The fundamental aspects of locally linear control synthesis are reviewed as applied to the synthesis of the control and the

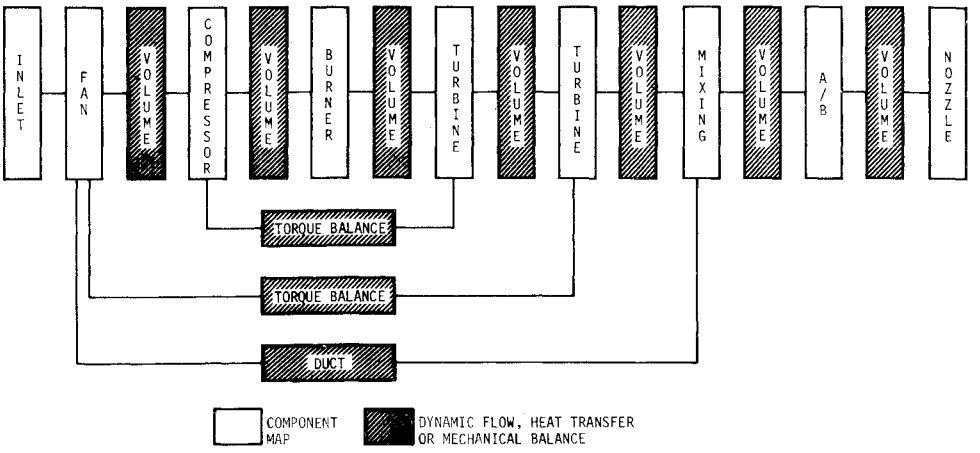

Fig. 1 F100 nonlinear simulation consisting of static component characteristics connected by dynamical blocks.

fundamental requirements of the control structure. The engine may be modeled conceptually as a nonlinear time-invariant dynamical system utilizing fundamental aerodynamic principles as follows:

$$\dot{x}=f(x,u,\theta) \tag{1}$$

$$y=h(x,u,\theta) \tag{2}$$

where n states x, m controls, u, p outputs, y, and q parametric variables θ, as well as the detailed nonlinear dynamics $f(.,.,.)$ and measurements $h(.,.,.)$, are modeled by the designer to achieve his purpose most expediently. For engine development, detailed digital simulations including thorough component maps and experimentally correlated gas path equations are utilized as in the F100 transient simulation deck.[12] These programs are too complex for control synthesis but are useful in evaluating a candidate design.

Locally linear models can be generated from nonlinear simulations[10] or experimentally from engine data via system identification, e.g., Ref. 13. These models are valid in the neighborhood of an equilibrium point (x_0,u_0,θ_0) and describe perturbation motion, δx, δu, away from equilibrium. These models are represented as follows:

$$\delta\dot{x}=F\delta x+G\delta u \tag{3}$$

$$\delta y=H\delta x+D\delta u \tag{4}$$

where, in principle,

$$F=\frac{\partial f(x,u_0,\theta_0)}{\partial x}\Big|_{x=x_0} \tag{5}$$

δx and δu will be rewritten as x, u in the remainder of this paper.

Figure 1 shows a schematic representation of the F100 digital transient simulation. Each dynamical element represents two or more states, and the entire linear model contains 16 state elements (Fig. 2). The linear model can be reduced in order to include only practically measurable elements and only important dynamics relative to the control objective.

$$\left[\begin{array}{c} x_1 \\ \hline x_2 \end{array}\right]=\left[\begin{array}{c|c} T_{11} & T_{12} \\ \hline T_{21} & T_{22} \end{array}\right]\left[\begin{array}{c} z_1 \\ \hline z_2 \end{array}\right] \tag{6a}$$

$$\left[\begin{array}{c} \dot{z}_1 \\ \hline \dot{z}_2 \end{array}\right]=\left[\begin{array}{c|c} \Lambda_1 & 0 \\ \hline 0 & \Lambda_2 \end{array}\right]\left[\begin{array}{c} z_1 \\ \hline z_2 \end{array}\right]+\left[\begin{array}{c} \Xi_1 \\ \hline \Xi_2 \end{array}\right] \tag{6b}$$

where x_1 and z_1 are the qth-order partition of states and modes, and x_2 and z_2 are the $(n-q)$th-order partition.

Various guidelines for making the appropriate partition will be discussed below, in which case the following equilibration relation can be attained approximately within the time frame of interest:

$$\dot{z}_2\approx 0 \tag{7}$$

If relation (7) is valid, the following relations hold:

$$\dot{x}_1=F_r x_1+G_r u \tag{8}$$

$$\left[\begin{array}{c} x_2 \\ \hline y \end{array}\right]=\left[\begin{array}{c} H^* \\ \hline H_r \end{array}\right]x_1+\left[\begin{array}{c} D^* \\ \hline D_r \end{array}\right]u \tag{9}$$

The formula for the reduced matrices follow from elementary matrix algebra.[11]

Thus, by assuming that $(n-q)$ modes are equilibrated, the nth order system (3) is reduced to the qth-order system (8) with q states and $p+n-q$ outputs. It should be noted also that the q retained states x_1 are chosen by the designer and possess the same physical identification in Eqs. (3) and (8) as long as Eq. (7) is approximately valid.

The partitioning of the system is dependent upon the control designer's estimate of the frequency range of the control function. For example, this F100 controller was designed primarily to modulate thrust in transient and steady-state operation. The response frequency range extends from 0 to about 10 rad/s, which is the bandwidth of the primary (fuel flow) actuator. The frequency range would be significantly different if, for example, the controller were designed to modulate compressor surge margin with a high-bandwidth, variable-area turbine actuator. The implication is that all eigenvalues significantly outside the bandwidth of interest are in equilibrium during the motion and may be partitioned with the $(n-q)$ eliminated roots.

A special situation occurs when a state is nearly parallel to a single modal direction. If the outputs are not affected significantly by the particular element, then the state and associated dyanmics can be removed from the design model without affecting behavior important to the control synthesis. Figure 3 shows the normalized eigenvectors associated with two eigenvalues for the F100 engine lying in the bandwidth of control. These modes are associated with temperature lag states at the turbine inlets. Examination of the thrust output equation shows that these states have a relatively small contribution. Thus, for control design purposes, the two states and the associated modes can be eliminated.

We have shown a number of techniques for choosing $(n-q)$ modes that can be eliminated, along with a group of states.

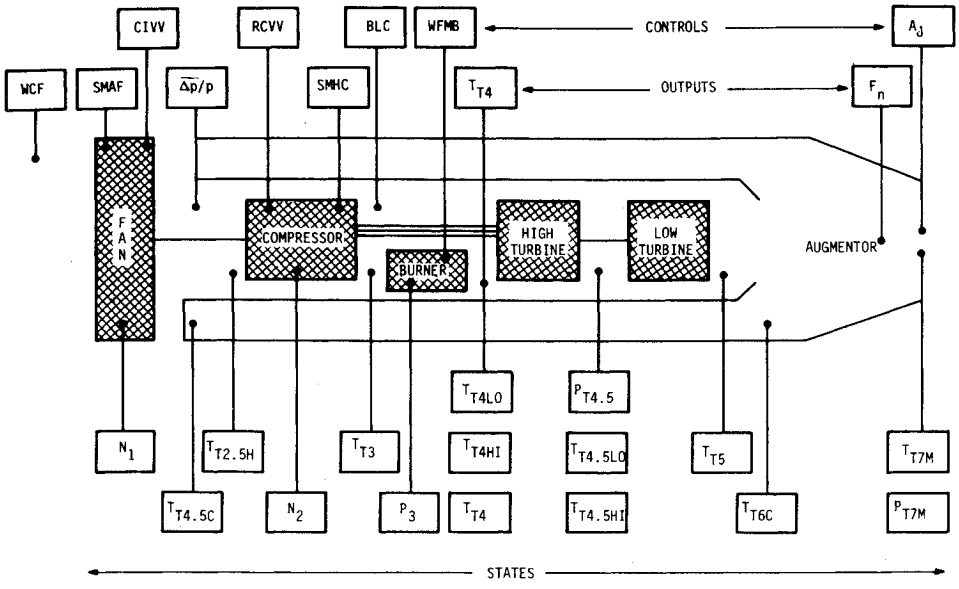

Fig. 2 States, outputs, controls modeled in F100 linear equations generated from nonlinear simulation.

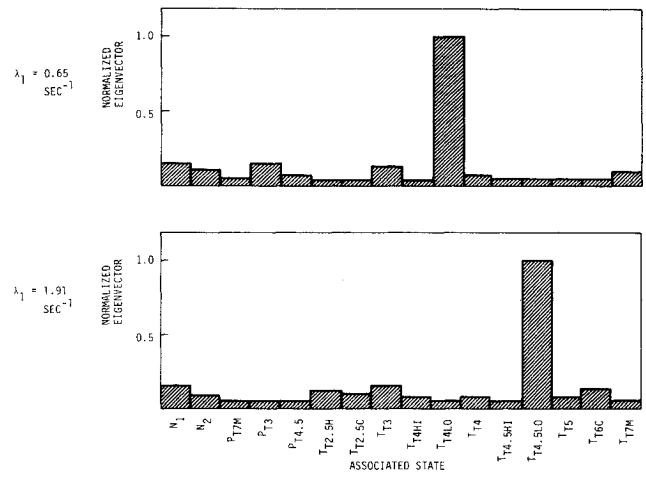

Fig. 3 Two uncoupled states/modes in the F100 turbofan.

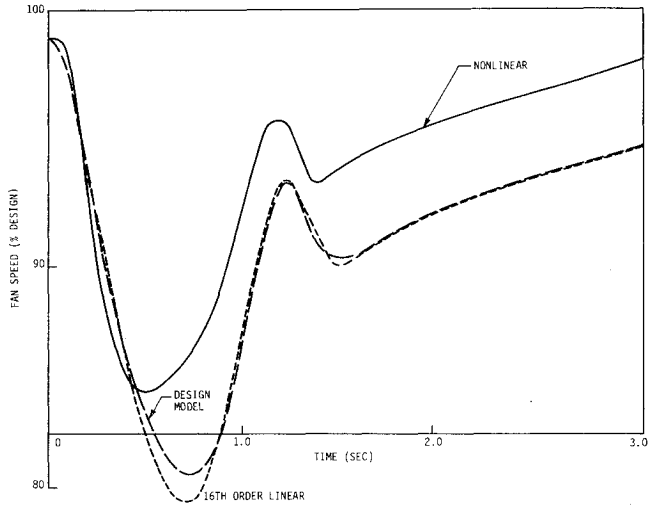

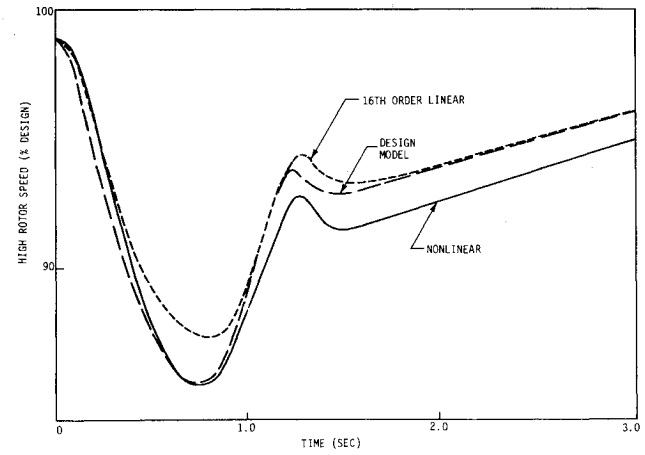

Fig. 4 Comparison of linear and nonlinear F100 engine model response.

The choice of the retained q states is somewhat arbitrary, depending on convenient measureables as well as the dependence of important output quantities. The model decomposition can be used to assure that the chosen q states strongly span the controlled subspace (T_{11} invertible and well conditioned). With this partition and associated reduction, the resulting system will represent a controllable design model.

For the F100, the behavior of the design model vis-a-vis the sixteenth-order linear system and nonlinear simulation is shown in Fig. 4. The reduction was performed on the linear system equations in each region of the operating envelope to provide a set of design models used in the optimal regulator synthesis. The total procedure to arrive most efficiently at multivariable designs requires the utilization of a blend of techniques incorporating frequency and time domain analysis and modern and classical control concepts.

Given the linear design model, [Eq. (8)] and the state/control performance index,

$$J=\frac{1}{2}\int_0^\infty (x^TAx+u^TBu)\,dt \tag{10}$$

or the output performance index,

$$J=\frac{1}{2}\int_0^\infty (y^TA^*y)\,dt \tag{11}$$

the deterministic, steady-state optimal controller to minimize J for arbitrary initial conditions about a fixed set point is given by the following state variable regulator control law:

$$u=u_0+C(x-x_0) \tag{12}$$

$$C=-B^{-1}G^TS \tag{13}$$

where u_0, x_0 are a consistent equilbrium reference point for the nonlinear plant, namely,

$$0=f(x_0,u_0) \tag{14}$$

where $f[x(t),u(t)]$ describes the nonlinear engine behavior exactly. The matrix S is given by the positive definite solution of the algebraic Ricatti equation [for Eq. (10)]

$$0=SF+F^TS+A-SGB^{-1}G^TS \tag{15}$$

and by a comparable form for Eq. (11). The solution is calculated numerically by integration of the matrix Riccati differential equation to steady-state or, more efficiently, by the eigenvector decomposition method.[15] The optimality of such regulators is given in terms of a fixed set point. However, with reasonable choices of weighting parameters, system response is not degraded for varying set-point inputs.

The state or output weightings can be constructed initially from physical reasoning. Alternately, if it is desired to alter the dynamic response in terms of time domain specifications (e.g., rise time or damping), state weightings on the variables most nearly associated with the mode to be controlled are chosen. For example, to increase the closed-loop frequency of the high-rotor-speed response root, weight on the high-rotor-speed state is chosen. State variables and output quantities often are related physically. Control of the state is then equivalent to control of the output. In this case, the need for explicit output weighting is removed. For example, engine thrust, an output, and augmentor pressure, a state, have nearly the same modal coefficient representation. Thus, weighting P_{T6} results in direct control of thrust response. Such considerations can give the designer a foundation for the initial quadratic weighting matrix selection.

If the number of control requirements are represented in the performance index simultaneously, it is probable that the initial design will be unacceptable in some way. Often, the unacceptable nature of the behavior can be linked directly to a particular closed-loop root and modal response vector. For example, thrust overshoot can be linked to a $P_{T6}-N_1$ complex pair in the closed-loop root constellation, as determined by an examination of the eigensystem. It is clear that the weights on either N_1 or P_{T6} or both must be adjusted so that the damping is increased. Sensitivities of the closed-loop locations to changes in weighting matrix elements can be calculated from decomposition of the Euler-Lagrange system used to solve the algebraic Riccati equation (15). For the decomposition,

$$HT=T\Lambda \tag{16}$$

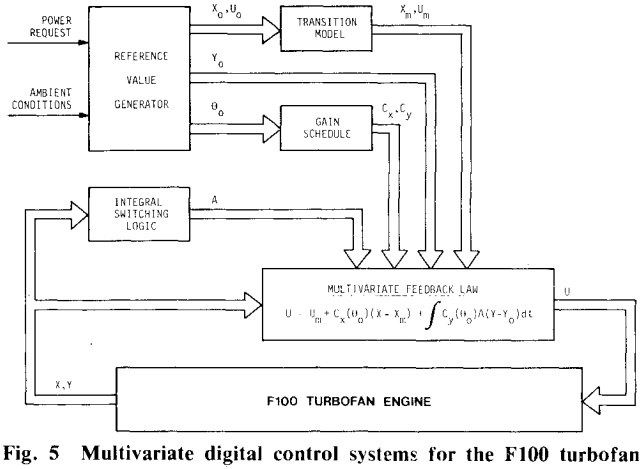

Fig. 5 Multivariate digital control systems for the F100 turbofan engine.

with Λ diagonal and H the dynamics of the Euler-Lagrange system; it can be shown[14] that

$$\frac{\partial\Lambda}{\partial\theta_i}=T^{-1}\frac{\partial H}{\partial\theta_i}T \tag{17}$$

$$\frac{\partial\Lambda}{\partial\theta_i}=\text{diag}\left\{\frac{\partial\lambda_j}{\partial\theta_i}\right\} \tag{18}$$

is the sensitivity of the eigenvalue location to a change in the weighting. The matrix $\partial H/\partial\theta$ normally consists of 1's and 0's, and the similarity transformation is available from the optimal controller solution. Utilizing Eq. (17), the correct weight change to alter the closed-loop pole locations is evaluated easily. Successive use of modal weighting sensitivity and time domain simulation will result in the quick convergence to a design with acceptable regulator performance.

Functional Description of Controller

Figure 5 shows a schematic representation of the digital controller. Each functional component of the system produces an element of the multivariate feedback law. The feedback law itself represents an optimal regulator structure with integral trims for steady-state accuracy and a model following implementation to prevent saturation during transients. Each element of the control law will be described relative to the F100 implementation, and the synthesis procedure for each block will be reviewed briefly.

Reference Value Generator

The control law is written for state and control perturbations about an equilibrium condition. The equilibrium conditions must be derived approximately by the controller given the requested power level, altitude, Mach number, engine face pressure, and temperature. Because of manufacturing tolerances and engine aging, an exact expression for these quantities is not possible. Inaccuracies in the scheduled reference values normally would cause steady-state "hand-offs" unless compensated with an integral trim action. Small inaccuracies do not degrade transient performance, and, indeed, the feedforward structure allows lower regulator feedback gains and the associated model parameter insensitivity of the control.

The reference schedules are produced by calculating the thermodynamic equilibrium associated with a given control vector. The manufacturer-specified steady-state condition[10] requires zero bleed flow and scheduled compressor geometry. Two degrees of freedom are left to attain desired thrust (power level) at a particular flight point. A constrained minimization can be performed to determine the required fuel flow and jet area to achieve requested thrust while optimizing a free variable, e.g., fuel consumption or surge margin, and respecting all engine structural limits. For comparison purposes, in the F100 controller, schedules were generated to match the production control operating point at each power level and flight point.

A representative group of subsonic and supersonic flight points was chosen, and the engine equilibrium points were calculated. Nondimensionalized quantities were utilized to fit approximate reference points with minimum complexity. The regulator is tolerant of the schedule errors and produces smooth transient responses without an overly complex implementation.

Transition Model

When a large transition in power is requested by the pilot, the perturbation character assumed in the regulator design is lost. A large change in the reference state vector will cause large commanded inputs, tending to saturate actuators and

produce significantly nonlinear behavior. The regulator can be used to track a compatitible trajectory taking the system for one state to another. Exact calculation of such trajectories is complex,[7] and their practical implementation has not been investigated. A first-order approximation to an achievable state trajectory can be calculated directly from the linearized models [Eqs. (3) and (4)]. In this case, it is assumed that

$$\dot{x} = R_x = \text{const} \tag{19}$$

and, allowing for various controllability constraints, a consistent set of equilibrium state and control rates R_x, R_y can be calculated if a particular set of ouput rates is specified. The nonlinear trajectory $[x_m(t),\ u_m(t)]$ then is approximated as follows:

$$x_m(t) = x_m(t_0) + R_u t \tag{20}$$

$$u_m(t) = u_m(t_0) + R_u t \tag{21}$$

where the transition is terminated when the new reference point is reached. The rates are derived from parametric fits of values calculated at each flight/power point.

In the F100 implementation, rates were calculated of low, middle, and high power. In the latter two cases, desired thrust and turbine inlet temperature rates characteristic of the engine were chosen. At low power, thrust and either burner pressure or surge margin rates were specified, depending on the flight condition, in order to specify adequate acceleration surge margin or eliminate burner pressure undershoot. Figure 6 shows the response of the nonlinear digital simulation to a large-power-level modulation. Engine state and trajectory time histories are shown, along with error terms in the regulator portion of the control law. The transition model prevents large error terms from saturating actuators during gross transients while still providing stiff regulation near steady-state conditions.

Gain Schedule

The dynamic response of the engine is affected strongly by the air mass flow. Power level, altitude, and Mach number

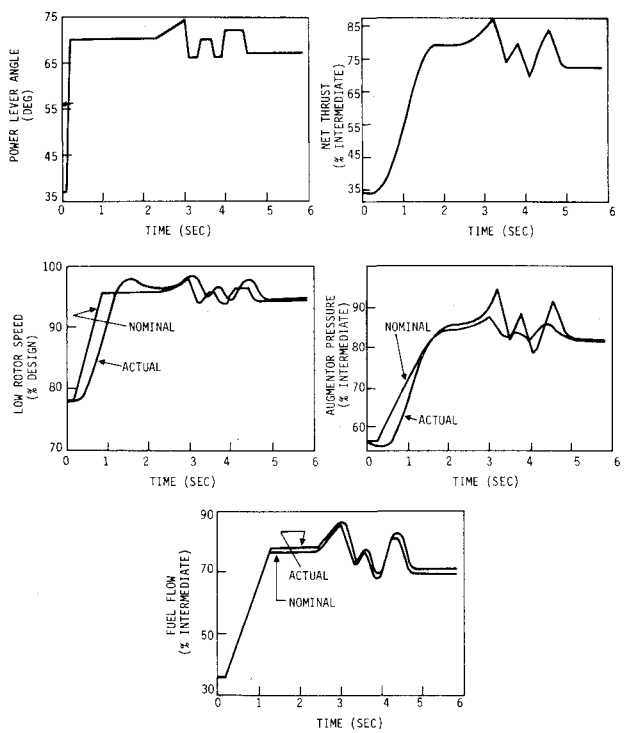

Fig. 6 Nonlinear simulation response to large power transient at sea-level static conditions.

determine this mass flow and the response. The linearized control synthesis procedure produces regulator gains that control the engine satisfactory in the neighborhood of the design flight/power point. To implement a continuous envelope-wide controller, the gains must be varied as the system makes the transition from one condition to another.

There is no precise analytical relationship between gains at neighboring linearization points. Although engine time constants can be modeled as functions of the ambient conditions, the performance index is chosen by the designer to satisfy specifications particular to the flight point. For example, a function of ambient variables will not correlate exactly the gain elements between sea-level static idle conditions, where thrust stability is weighted heavily, and subsonic altitude idle, where burner pressure is the dominant state weight. The procedure adopted for the F100 implementation approximately fit important gain elements with univariate functions of the engine face density and rotor speed. The former variable accounts for altitude effects, while the latter schedules the power condition. Dominant gain elements are determined by assessing the closed-loop eigenvalue sensitivity of the system to each gain element[9] and eliminating those that do not affect closed-loop response.

Integral Switching Logic

The design philosophy of aircraft turbine engines dictates that steady-state performance is obtained at various flight conditions when a particular physical limit is held exactly (see Fig. 7). For example, sea-level static takeoff thrust for the F100 is defined as the thrust obtained at the maximum allowable turbine inlet temperature. At lower power levels, the engine operation should cause the airflow and low rotor speed to attain predetermined values for optimum efficiency. At altitude conditions, the minimum burner pressure defines engine idle. Inlet airflow requirements and burner burst pressure determine operating conditions at some supersonic flight points.

The engine set point is a group of reference values of states and controls which the engine must attain exactly in steady state. These values define the equilibrium point. Since the F100 has set-point vectors whose elements change with flight and power conditions, a switching structure from trim control is required.

Given the design model [Eq. (3)] and the linear quadratic regulator design [Eq. (12)], the closed-loop response to additive control inputs may be written as follows:

$$\dot{x} = (F + GC)x + Gu' \tag{22}$$

where

$$u = Cx + u' \tag{23}$$

and u' is the additional control input. If the trim responses (i.e., the integral control time constants) are decoupled spectrally from the transient [i.e., time constants of Eq. (22) roots], then the following should be approximately valid:

$$\dot{x} \approx 0 \tag{24a}$$

$$x = -(F + GC)^{-1} Gu' \tag{24b}$$

$$y = [-(H + DC)(F + GC)^{-1} G + D]u' \tag{24c}$$

$$y \triangleq H^* u' \tag{24d}$$

The output vector y is chosen as m quantities, which must be held in steady state to their reference values. (Controllability is assured, then, if H^* is invertible.) The trim integrations provide the system dynamics, namely,

$$\dot{b} = y \tag{25a}$$

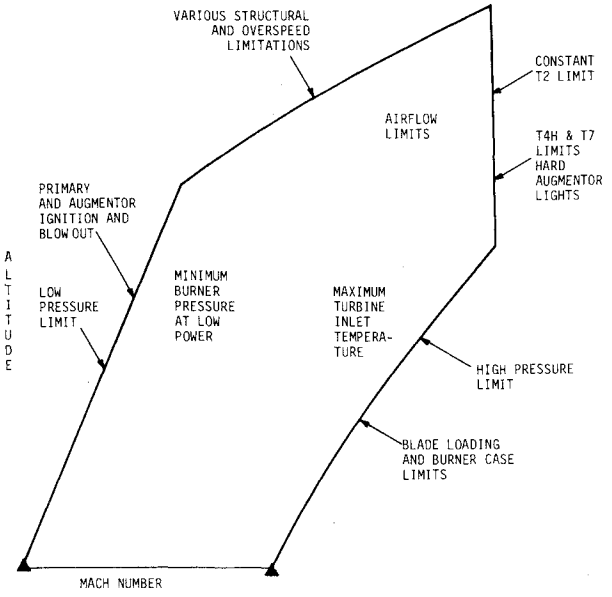

Fig. 7 F100 operating envelope and constraining physical limits.

The control law is designed:

$$u' = C_b b \tag{25b}$$

and the full controller is implemented:

$$u = Cx + \int C_b y \mathrm{d}t \tag{26}$$

where the elements of y and C_b can be switched arbitrarily while maintaining a continuous control time history.

The design of the control law C_b could be performed with a single application of the regulator synthesis procedure. However, because the elements of the y vector change according to limit conditions and control saturations, a complete design for all combinations of error vectors would require an extremely large number of C_b matrices stored in the controller.

The classical approach is to ignore various couplings in H^*, and the integral control can be designed on a loop-by-loop basis. For each output,

$$\dot{b}_i = h_i^{*T} u' \tag{27}$$

If control weightings are chosen to represent the amount of control $u'_{j_{\max}}$ which should be used to trim the output error y_i as follows:

$$B_{jj} = 1/(u_j)^2_{\max} \tag{28}$$

then the optimal single-loop output regulator can be designed to place the spectrally separated trim root at $s = -\lambda$. The gain for this system is

$$C_{b_i} = -\lambda B^{-1} h^*_i / h_i^{*T} B^{-1} h^* \tag{29}$$

The full gain matrix C_b is constructed as follows:

$$C_b = [C_{b_1} \mid C_{b_2} \mid \cdots \mid C_{b_r}] \tag{30}$$

where columns are chosen corresponding to the appropriate set point and number of unsaturated controls. Equation (30) represents a single matrix that can accommodate any subset of output errors as long as a suitable set of actuators is available. The drawback of such a procedure is that the precise eigenvalue location of the trim root system is determined only approximately because of the neglected cross-couplings in Eqs. (24). The problem can be minimized if the weightings are chosen [Eq. (28)] such that each control is used primarily to modulate a single output error. The closed-loop eigensystem must be determined to verify suitable root locations for the trim and transient system combined. Further iterations may be required.

Alternately, if the closed-loop trim system

$$\dot{b} = H^* C_b b \tag{31}$$

is chosen such that H^*C_b is upper triangular, then any row and column of C_b can be deleted without altering the remaining closed-loop dynamics. Also, it is possible to replace a single row of Eq. (31) arbitrarily without affecting the remaining dynamics. The upper triangular structure and eigenvalue placement determined $(m)(m+1)/2$ constraint equations. The remaining $(m)(m-1)/2$ free elements of C_b can be chosen as zero, or a quadratic regulator construction in Eq. (29) can be used to resolve the ambiguity.

Either method just described produces a single $m \times r$ gain, where r is the total number of possible output quantities. If l controls are saturated, m-l elements of the r output quantities can be chosen for trim. The control law then is implemented as in Eq. (26), with the l rows corresponding to the saturated actuators deleted from the matrix. The control is switched when an actuator saturates (delete a row and column), an engine limit must be accommodated (a column is replaced), or the error term associated with the saturated control will tend to unsaturate the control (add the row and column). The implementation produces an extremely simple structure for trim and transient control action which can accommodate various engine limits and control saturation, as well as obtain rated engine performance accurately throughout the envelope.

In the F100 implementation, the steady-state requirements are to have the compressor bleeds closed, vanes and stators tracking the optimum component efficiency schedules, and fuel flow and jet area adjusted to yield operating line performance without limit exceedance. Three elements of the set-point vector are the vane, stator, and bleed schedules. These error terms always are integrated unless they are driven transiently into saturation. To avoid integrator windup due to this uncontrollable situation, the appropriate error is switched out until the transient command tends to cause the control to unsaturate. The remaining two elements of the set point are, normally, scheduled low rotor speed and an averaged fan exit total to static pressure difference $\Delta p/p$. The $\Delta p/p$ error term is eliminated if the jet area saturates. If burner pressure or turbine inlet temperature limits are reached, these terms are substituted for low rotor speed in the control law. The switching logic provides smooth and controlled engine transitions in power and flight condition.

The F100 multivariable control has been implemented on a general-purpose digital computer (SEL 810B) and evaluated on a hybrid computer simulation[16] of the engine at the NASA Lewis Research Center. Testing of the engine control is scheduled presently for an altitude cell.

A multivariate control system for the F100 turbofan engine has been described. The theoretical foundations of locally linearized control have been reviewed, and it has been shown that the resulting form of the control law dictates the implemented control structure. Basic components of the control include 1) a reference value generator for deriving an approximate equilibrium state and control vector, 2) a transition model to produce compatible reference point trajectories during gross transients, 3) gain schedules for producing feedback terms appropriate to the flight condition, and 4) the integral switching logic to produce acceptable steady-state performance without engine operating limit exceedance. The design philosophy for each component is described and the details of the F100 implementation presented. It is concluded that the structure is sufficiently general to be applied to most

modern aircraft turbine engine systems to produce smooth transition control and accurate steady-state regulation.

Acknowledgments

This work was sponsored by the U.S. Air Force, Aero Propulsion Laboratory (AFAPL), Wright-Patterson Air Force Base, Dayton, Ohio, and NASA Lewis Research Center, Cleveland, Ohio, under Contract No. F33615-75-C-2053. Charles Skira is the AFAPL Technical Monitor.

References

[1]Stone, C.R., Miller, N.E., Ward, M.D., and Schmidt, R.D., "Turbine Engine Control Synthesis," Air Force Aero Propulsion Lab., AFAPL-TR-75, March 1975.

[2]Seitz, W.R., "Integrated Flight/Propulsion Control by State Regulation," The Bendix Corp., 1975; also AIAA Paper 75-1075, Boston, Mass., Aug. 1975.

[3]Michael, G.J. and Farrar, F.A., "An Analytical Method for the Synthesis of Nonlinear Multivariable Feedback Control," Office of Naval Research, Dept. of the Navy, AD-762-797, June 1973.

[4]Beattie, E.C., "Control Mode Studies for Advanced Variable-Geometry Turbine Engines," Pratt & Whitney Aircraft, Commercial Products Div., United Aircraft Corp., Air Force Aero Propulsion Lab., AFAPL-TR-75-7, Nov. 1974.

[5]Weinberg, M.S., "A Multivariable Control for the F100 Engine Operating at Sea Lavel Static," Aero Force Aeronautical Systems Div., ASD-TR-75-28, Nov. 1975.

[6]Merrill, W.C., "An Application of Modern Control Theory to Jet Propusion Systems," TM X-71726, May 1975.

[7]Teren, F., "Minimum Time Acceleration of Aircraft Turbofan Engines," NASA TM X73624, July 1977.

[8]DeHoff, R.L. and Hall, W.E., "Jet Engine Systems Modeling—State Space Techniques and Modeling for Control," *Advances in Control and Dynamic Systems,* Vol. XIV, edited by C.T. Leondes, Academic Press, New York, 1977.

[9]De Hoff, R.L. and Hall, W.E., "Design of Multivariable Controller for an Advanced Turbofan Engine, *Proceedings of the 1976 IEEE Conference on Decision and Control,* Clearwater Beach, Fla., Dec. 1976, p.1002.

[10]Miller, R.J. and Hackney, R.D., "Research on F100 Multivariable Control," Air Force Aero Propulsion Lab., AFAPL-TR-76-74, AFAPL Contract F33615-75-C-2048, Final Rept. for June 1, 1975-Aug. 31, 1976.

[11]DeHoff, R.L. and Hall, W.E., "Multivariable Design Procedures for the F100 Turbofan Engine," AFAPL-TR-77-35, Final Rept. Contract F33615-75-C-2053, Jan. 1, 1977.

[12]"F100-PW-100 (3) Transient Engine Simulation Deck," Pratt & Whitney Aircraft Government Products Div., Fr-6014, Oct. 15, 1973.

[13]De Hoff, R.L. and Hall, W.E., "System Identification Principles Applied to the Control and Fault Diagnosis of the F100 Turbofan Engine," *Proceedings of 1977 Joint Automatic Control Conference,* San Francisco, Calif., June 1977.

[14]Porter, B. and Crossley, R., *Modal Control Theory and Applications,* Barnes and Noble, London, 1972.

[15]Bryson, A.E., and Hall, W.E., "Optimal Control and Filter Synthesis by Eigenvector Decomposition," Stanford Univ., Dept. of Aeronautics and Astronautics, Rept. 436, Nov. 1971.

[16]Szuch, J.R. and Seldner, K., "Real-Time Simulation of F100-PW-100 Turbofan Engine using the Hybrid Computer," NASA TM X-3261, Aug. 1975.